NASA Technical Memorandum 58274

Implicit Methods for Computing Chemically Reacting Flow

Chien-peng Li

September 1986

National Aeronautics and
Space Administration

Lyndon B. Johnson Space Center
Houston, Texas

NASA Technical Memorandum 58274

Implicit Methods for Computing Chemically Reacting Flow

Chien-peng Li

Lyndon B. Johnson Space Center

Houston, Texas

N A S A

National Aeronautics and
Space Administration

Scientific and Technical
Information Branch

1986

CONTENTS

FIGURES

1. Introduction

Modeling the inviscid air flow and its constituents over a hypersonically flying body requires a large system of Euler and chemical rate equations in three spatial coordinates. In most cases, the simplest approach to solve for the variables would be based on explicit integration of the governing equations. But the standard techniques are not suitable for this purpose because the integration step size must be inordinately small in order to maintain numerical stability. The difficulty is due to the stiff character of the difference equations, as there exists a large spectrum of spatial and temporal scales in the approximation of physical phenomena by numerical methods. For instance, in the calculation of gradients caused by shock and by cooled wall on a coarse grid, unchecked numerical errors eventually will lead to violent instability, and in calculations of species near chemical equilibrium, a small error in one species will give rise to a large error in the source term for other species. Despite the different nature of the stiffness in a complex system of equations, the most effective approach is believed to be implicit integration. The step increment is no longer dictated by the stability criteria for explicit methods, but instead is dictated by the degree of linearization introduced to the governing equations and by the order of desired accuracy. The linearization is enacted by means of Jacobian matrices, resulting from the differentiation of the flux as well as the rate production terms with respect to dependent variables. The backward Euler scheme is then applied to discretize the partial differential equations and to convert them into a system of linear difference equations in vector form. As this particular approach has the A-stable property, it is the one recommended by Lomax and Bailey[1] for one-dimensional nonequilibrium flow studies. However, in the practice of solving flow problems in multidimensions, it was not clear then how to deal with the mammoth size of the sparse block matrix equations. The implementation of an implicit method in the solution procedure could be as prohibitively expensive as a modified Runge-Kutta method.[2]

2. Formulation

In view of the drawbacks associated with the implicit methods, other concepts have been evolved to avoid using the fully coupled approach. The most notable concepts probably are the hybrid explicit-implicit techniques that focus on the minimization of the stiffness due to the chemical production[3-4] and the time-split explicit method devised in such a manner that the flow and species equations are integrated separately according to the stability criteria of each.[5] These plausible ideas have provided limited success in two-dimensional problems, for which the flow equations are not stiff. The dilemma in regard to the unrestricted stability conditions and the excessive manipulation of a matrix-vector equation may be resolved now by taking a different path in seeking an efficient method.

The objective of the research reported herein is to evaluate the efficiency and robustness of two variants of an implicit method that has recently been developed to investigate the complete flowfield around an entry vehicle. The most challenging aspect of nonreacting flow computation was the generation of a computational grid so as to allow a single data set structure for both shock layer and trailing wake in one zone. The Euler equations were cast in the domain between the wall and the outer surface consisting of the bow shock and were solved by a modified version of the ADI factorization technique.[6] The methodology can be extended to consider reacting species in several ways; namely, coupled flow and species, decoupled flow from species and simultaneous species solution, and decoupled successive

species solution. The differences among the three approaches are mainly in the degree of linearization and the ensuing amount of computation. The coupled approach would be the favorable one to use if the initial conditions are close to the final solution and the temporal accuracy is critical. The last two approaches are more appealing whenever the final solution is obtained after a reasonable, economical number of iterations. In the hypersonic flowfield with large subsonic regions surrounding the body, the initialization is at best very crude. Hence, the issue of efficiency is not as important as the robustness issue. Besides, the third approach has the potential of being the least computationally intensive method as the ionization is considered (11 vs 7 species).

3. Outline of the Decoupled Methods

The ideas can be elucidated by the one-dimensional problem having two species.

$$U_t + F_x + R = 0 \tag{1}$$

where

$$U = \begin{bmatrix} \rho \\ \rho u \\ \rho\varepsilon \\ \rho C_M \\ \rho C_A \end{bmatrix}, \quad F = \begin{bmatrix} \rho u \\ \rho u^2 + p \\ (\rho\varepsilon + p)\,u \\ \rho C_M u \\ \rho C_A u \end{bmatrix}, \quad R = \frac{A_x}{A} \begin{bmatrix} \rho u \\ \rho u^2 \\ (\rho\varepsilon + p)\,u \\ \rho C_M u - \rho\omega_M \\ \rho C_A u - \rho\omega_A \end{bmatrix}$$

and A is the duct area; the subscripts M and A refer to molecular and atomic species respectively; and ω is the production term. Standard notation is used otherwise.

An alternate equation equivalent to Eq. (1) is

$$V_t + AV_x + S = 0 \tag{2}$$

where

$$V = \begin{bmatrix} \rho \\ u \\ e \\ C_M \\ C_A \end{bmatrix}, \quad A = \begin{bmatrix} u & \rho & 0 & 0 & 0 \\ ge/\rho & u & g & 0 & 0 \\ 0 & p/\rho & u & 0 & 0 \\ 0 & 0 & 0 & u & 0 \\ 0 & 0 & 0 & 0 & u \end{bmatrix}, \quad S = \frac{A_x}{A} \begin{bmatrix} \rho u \\ 0 \\ u(e + p/\rho) \\ -\omega_M \\ -\omega_A \end{bmatrix}$$

$$dU = PdV, \quad P = \begin{bmatrix} 1 & 0 & 0 & 0 & 0 \\ u & \rho & 0 & 0 & 0 \\ q & \rho u & \rho & 0 & 0 \\ C_M & 0 & 0 & \rho & 0 \\ C_A & 0 & 0 & 0 & \rho \end{bmatrix}, \quad q = 0.5\ u^2$$

It is readily seen from Eq. (2) that a weak relationship exists between (ρ,u,e) and (C_M,C_A). The loosely coupled property in P and A will be exploited further in the following section. Since neither Eq. (1) nor Eq. (2) is sufficient to describe the flowfield, two equations of T and p

$$T_t + \left[e_t - \sum_\ell \left(C_\ell\right)_t e_\ell\right] / \sum_\ell C_\ell\, e_\ell = 0 \tag{3}$$

$$p = \rho R T \sum_\ell C_\ell / M_\ell$$

also are needed. Relations of the conservation of mass concentration, C_ℓ, and of charges are used for more complicated chemistry.

The production term, $\omega_\ell = \omega_\ell(\rho,T,C_\ell)$, is proportional to $(C_\ell - C_{\ell e})/\tau$, where $C_{\ell e}$ is the equilibrium value and τ is the reaction rate. It can have astronomical value even when normalized by the flow resident time in some portion of the flow. To cope with such stiffness, its relationship with the dependent variable should be analyzed and included in the algorithm by means of a Taylor series expansion as follows:

$$\omega_\ell = \overset{\circ}{\omega_\ell} + \left(\frac{\partial \omega_\ell}{\partial C_m}\right)^\circ \Delta C_m + \left(\frac{\partial \omega_\ell}{\partial \rho}\right)^\circ \Delta\rho + \left(\frac{\partial \omega_\ell}{\partial e}\right)^\circ \Delta e \tag{4}$$

The superscript $^\circ$ denotes the known values, and Δ represents the difference between the present and the known values. By incorporating Eq. (4) to Euler's backward scheme, Eq. (2) is converted to difference form in shorthand notation.

$$M_i^k\, \Delta V_i^{k+1} + \Delta t\, \delta_x\left(A_i^k\, \Delta V_i^{k+1}\right) = RHS \tag{5}$$

where δ_x refers to the centered-difference operator, i is the index of the grid and

$$RHS = -\Delta t P^{-1}\left(\delta_x F_i^k + R_i^k\right)$$

$$M = \begin{bmatrix} 1 & 0 & 0 & 0 & 0 \\ 0 & 1 & 0 & 0 & 0 \\ 0 & 0 & 1 & 0 & 0 \\ \left(\omega_M\right)_\rho \Delta t & 0 & \left(\omega_M\right)_e \Delta t & 1 - \left(\omega_M\right)_{C_M} \Delta t & \left(\omega_M\right)_{C_A} \Delta t \\ \left(\omega_A\right)_\rho \Delta t & 0 & \left(\omega_A\right)_e \Delta t & \left(\omega_A\right)_{C_M} \Delta t & 1 - \left(\omega_A\right)_{C_A} \Delta t \end{bmatrix}$$

The appearance of M in Eq. (5) and of the partial derivatives in the elements of M serves the role of tempering the resultant ΔV_i. Simplifications can be made to M by neglecting off-diagonal elements or only those elements associated with $(\,)\rho$ and $(\,)e$. Then, Eq. (5) is effectively decoupled into two groups for flow and species variables.

M has two splitup versions as follows:

$$M_F = \begin{bmatrix} 1 & 0 & 0 \\ 0 & 1 & 0 \\ 0 & 0 & 1 \end{bmatrix}, \quad M_S' = \begin{bmatrix} 1 - \left(\omega_M\right)_{C_M} \Delta t & \left(\omega_M\right)_{C_A} \Delta t \\ \left(\omega_A\right)_{C_M} \Delta t & 1 - \left(\omega_A\right)_{C_A} \Delta t \end{bmatrix}$$

$$M_S = \begin{bmatrix} 1 - \left(\omega_M\right)_{C_M} \Delta t & 0 \\ 0 & 1 - \left(\omega_A\right)_{C_A} \Delta t \end{bmatrix}$$

It is interesting to note that, in the simplest version, M_S^{-1} multiplies the RHS and the operator δ_x and results in the reduction of the time increment Δt by a factor of $1 + |(\omega_i)_{Ci} \Delta t|$. Since each species equation is then integrated by a different Δt, this approach uses the same idea advocated in Li.[5]

Equation (5) is a tridiagonal block or scalar system of equations depending on the form of M for which the solution procedure is selected. It represents one of the three steps in solving three-dimensional problems. The truncation error of the method is $(\Delta t^2, \Delta x^3)$. By contrast, higher order explicit methods can be constructed by using

$$\Delta V_i^{k+1} = M_i^{-1} (RHS) \tag{6}$$

although Δt may be restricted to a narrow corridor of $\lambda \Delta t$, where λ is the largest eigenvalue of A.

4. Discussion of Results

The development of decoupled implicit methods was based on two body configurations of practical interest and under flow conditions that give rise to extreme levels of dissociation and ionization. The fully implicit method has not been implemented in a computer code

because it appears to be prohibitively costly for an 11-species model on today's scalar computer. The simultaneous species solver was used primarily to compare its performance with the less expansive successive species solver.

The first case was a sphere of $R_N = 0.328$ ft, at $M = 10$ and $h = 100$ kft. Some results of $M = 10$ reacting flow over the frontal portion of the sphere (table 3.16 in Belotserkoskiy[7]) were used to verify the accuracy of present results. In as much as the body is simple and the dissociation is weak, a coarse grid of 6×20 was found to be adequate.

Figure 1 shows the convergence history of the mass fraction of the oxygen molecule in terms of the maximum incremental and the stagnation values. As shown, both figures are needed to exhibit the realistic rate of convergence. The noticeably slow relaxation process in chemical nonequilibrium is indicative of the mutual interactions between the convection and the production of species allowed by the step size, $CN = 2$. Attempts to increase the Courant number to $CN = 4$ failed to control the growth of error; indeed, a wide band of fluctuation was observed in ΔC_{O_2}. After ΔC_{O_2} had reached and stayed at the level of truncation error, C_{O_2} began to converge at the forward stagnation point. Using the convergence history obtained from both methods, it was estimated that the successive method is a factor of two slower.

Figure 2 presents the temperature and species distributions across the shock layer in three angular orientations: $\theta = 0, \pi/2$, and π. An excellent agreement is found in temperature, but discrepancies are seen in the species distributions. As pointed out in Li, [5] the rate constants usually exert stronger influences on the species than on the temperature.

The second case investigated was an aerobrake of $R_N = 20$ ft at $M = 34.8$ and $h = 250$ kft. The computational grid, 13×36, was similar to that developed in Li[6] for nonreacting flow computations. A comparison of the convergence history between the simultaneous and the successive methods is shown in Fig. 3 for the nitrogen atom. The formal method has a faster rate in the first 100 iterations, but commands as many iterations as the latter method to reach the asymptotic value. The simultaneous method has produced a great deal of fluctuation that is atypical for flow with high levels of dissociation.

The successive method was slightly more efficient (by 15%) than the simultaneous method. Out of the total execution time, about 50% was spent to solve for the flow variables, 43% for the 5×5 ω_C matrix, and the rest of the execution time for the species. During each iteration, the analytical procedure determining ω and ω_C was called twice for each grid point such that no extra core was assigned to store them.

The temperature contours obtained for the two cases are exhibited in Fig. 4. A complete flowfield can be obtained with 200 to 400 iterations on the coarse grid laying between the wall and the outer surface.

Figure 5 illustrates the convergence history of C_N at the front and the rear stagnation points. This is the same aerobrake considered in case 2, but at a 20° angle of attack. The nonequilibrium flow in the shock layer changed little after 200 iterations, yet, in the near wake, probably more than 400 iterations were required to ensure convergence. Note that the stagnation value of C_N was lower than that predicted for the zero angle of attack case. Figure 6 gives the contour plot of Mach and e^- (no./cm^3) made on the pitch plane. The shear layer was not clearly visible because the grid of $13 \times 36 \times 6$ was quite coarse. The distribution of electrons displays three orders of magnitude difference between the shock layer and the wake.

5. Conclusion

It was found that the conventional implicit techniques can effectively reduce the stiffness associated with the chemical production term in the rate equations. The successive solution for the species was as stable as the simultaneous solution. The fact that reactive

Jacobians were used to scale down the time increment was essentially regarded as a means to separate the rate equations and to perform integrations according to individual reaction time. In summary, the numerical procedure consists of decoupling the flow from species equations, solving them by block and scalar tridiagonal procedures, respectively, and utilizing the factorization ADI technique to tackle two- or three-dimensional problems. The procedure is stable and the computation time of species varies linearly with the number of species. Significant reduction of computation time can be achieved by storing the reactive Jacobians and by updating them periodically in the coarse of iterations.

References

1. Lomax, H., and Bailey, H., NASA TN D-4109, 1967.

2. Treanor, C. E., *Math. Comp.*, Vol. 20, 1966, pp. 39-45.

3. Rakich, J. V., and Park, C., Symposium on Application of Computers to Fluid Dynamic Analysis and Design, Polytechnic Institute of Brooklyn Graduate Center, New York, 1973.

4. Widhopf, G. F., and Victoria, K. J., Symposium on Application of Computers to Fluid Dynamic Analysis and Design, Polytechnic Institute of Brooklyn Graduate Center, New York, 1973.

5. Li, C. P., *J. Spacecraft & Rockets*, Vol. 9, 1972, pp. 571-572.

6. Li, C. P., Inter. Symp. Computational Fluid Dynamics - Tokyo, 1985, or NASA TM-58269, 1985.

7. Belotserkoskiy, O. M., NASA TT F-453, 1967.

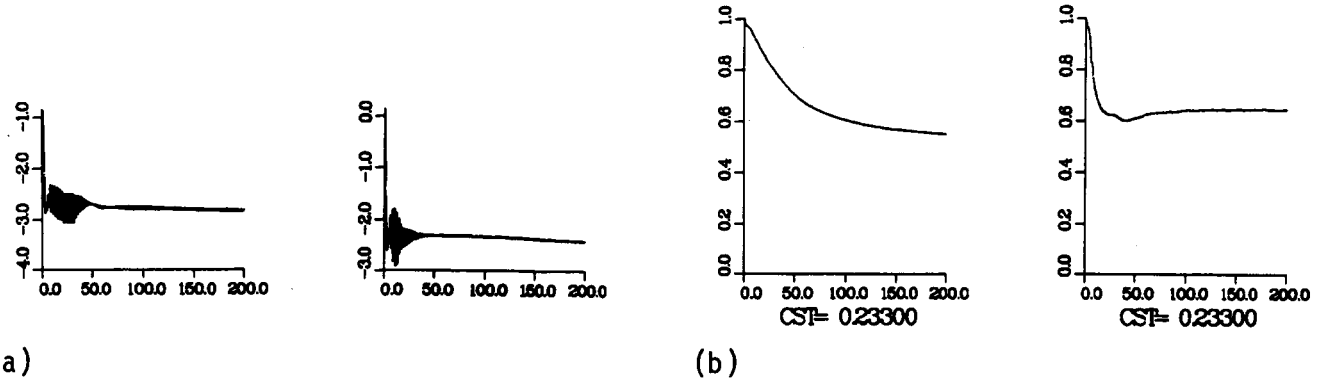

Fig. 1 Comparison of the convergence history between the simultaneous and successive solutions for case 1: (a) maximum value of the incremental C_{O_2}; (b) forward stagnation value of C_{O_2}, normalized by its maximum value.

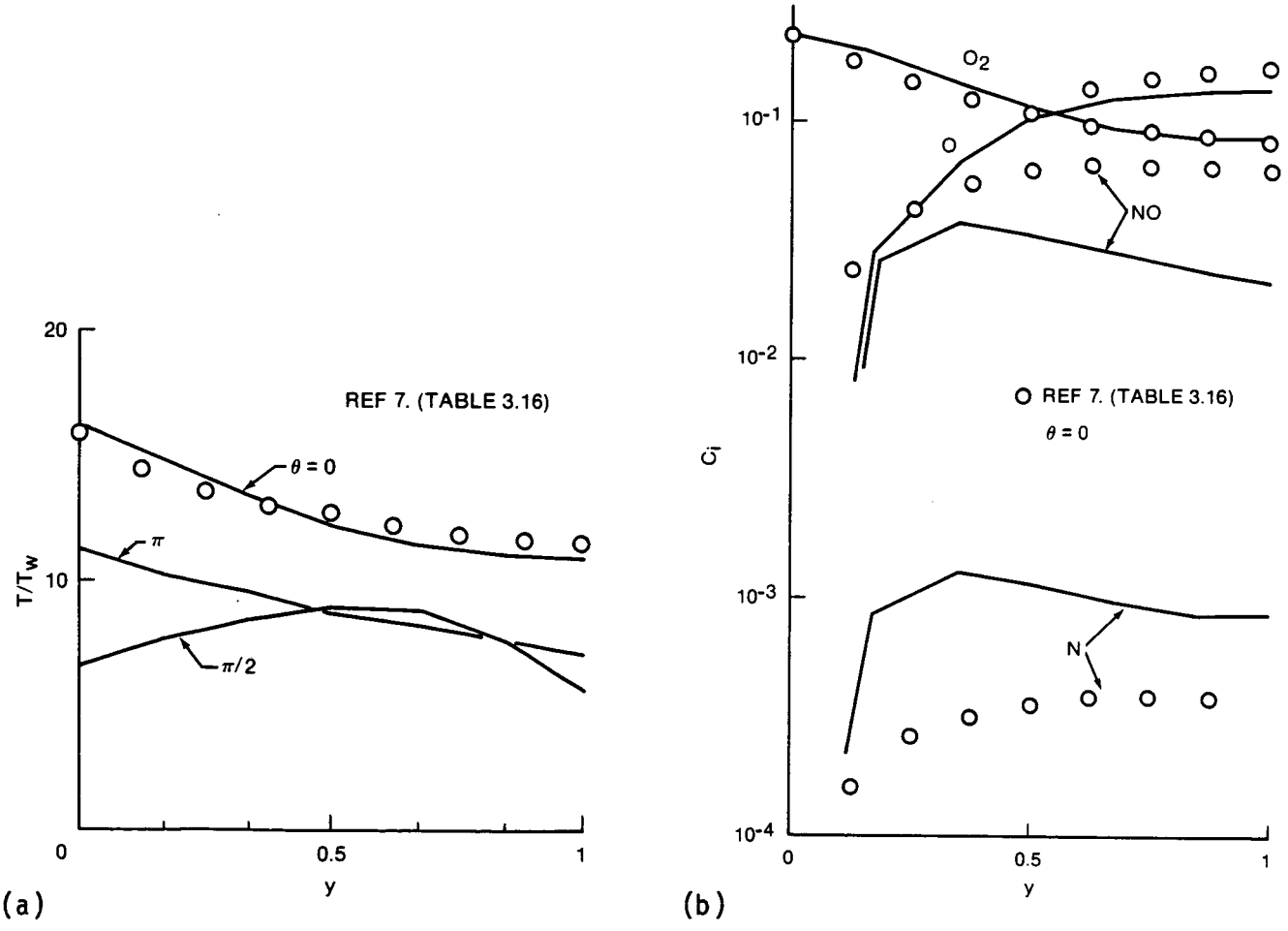

Fig. 2 Comparison of temperature and species mass fractions: (a) temperature distributions vs normalized distance from outer surface to wall; (b) species distributions along the forward stagnation line between shock and wall.

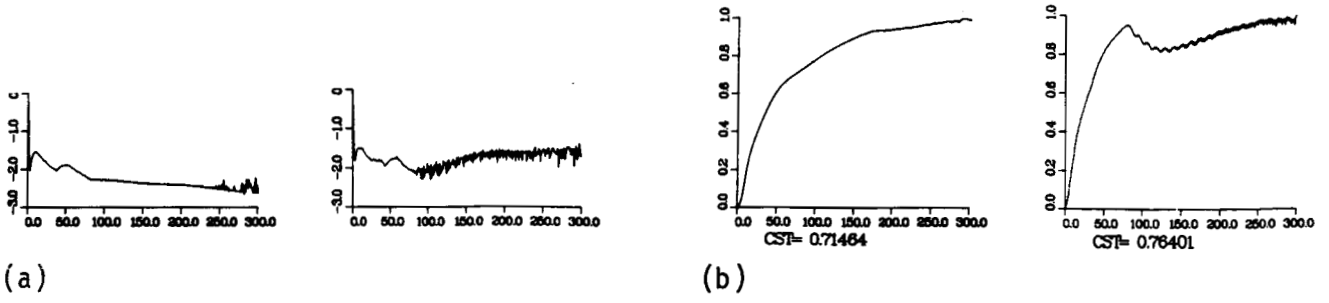

Fig. 3 Comparison of the convergence history between the simultaneous and successive solutions for case 2: (a) maximum value of the incremental C_N; (b) forward stagnation value of C_N, normalized by its normalized value.

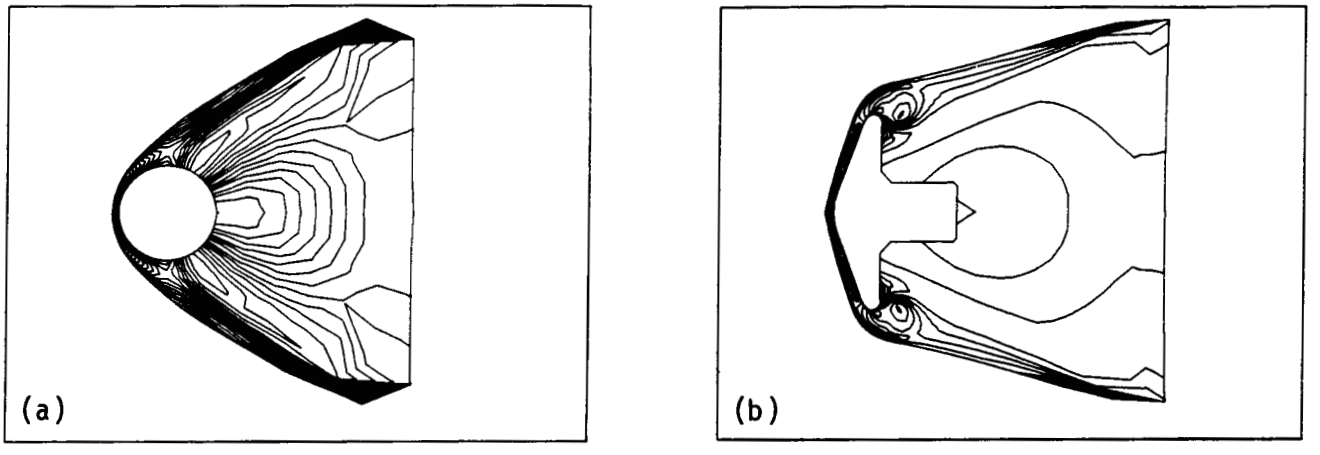

Fig. 4 Temperature contours for cases 1 and 2: (a) case 1; (b) case 2.

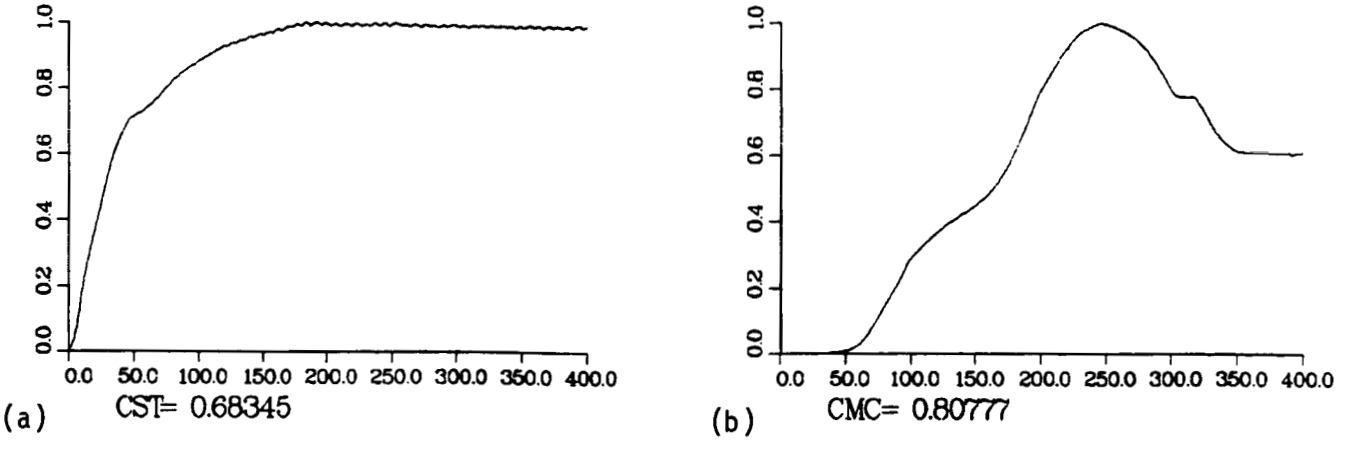

Fig. 5 Convergence history of case 2 at $\alpha = 20°$: (a) front stagnation value of C_N; (b) rear stagnation value of C_N. Both are normalized quantities.

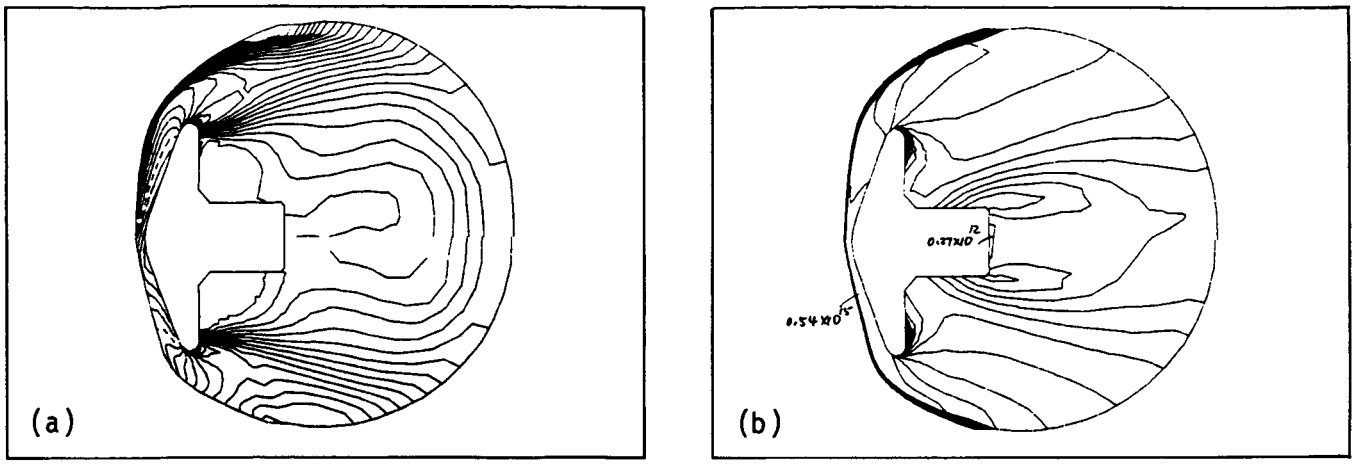

Fig. 6 Contours of Mach number and electron number density (dash line = sonic line): (a) Mach number; (b) e- (no./cm^3).

1. Report No.	2. Government Accession No.	3. Recipient's Catalog No.
NASA TM-58274		

4. Title and Subtitle	5. Report Date
IMPLICIT METHODS FOR COMPUTING CHEMICALLY REACTING FLOW	August 1986
	6. Performing Organization Code 569-85-00-00-72

7. Author(s)	8. Performing Organization Report No.
Chien-peng Li	S-554
	10. Work Unit No.

9. Performing Organization Name and Address	11. Contract or Grant No.
Lyndon B. Johnson Space Center Houston, Texas 77058	
	13. Type of Report and Period Covered Technical Memorandum

12. Sponsoring Agency Name and Address	14. Sponsoring Agency Code
National Aeronautics and Space Administration Washington, D.C. 20546-0001	

15. Supplementary Notes

Presented at the Tenth International Conference on Numerical Methods in Fluid Dynamics, Beijing, China, June 23-26, 1986

16. Abstract

The backward Euler scheme was used to solve a large system of inviscid flow and chemical rate equations in three spatial coordinates. The flow equations were integrated simultaneously in time by a conventional ADI factorization technique, then the species equations were solved by either simultaneous or successive technique. The methods were evaluated in their efficiency and robustness for a hypersonic flow problem involving an aerobrake configuration. It was found that both implicit methods can effectively reduce the stiffness associated with the chemical production term and that the successive solution for the species was as stable as the simultaneous solution. The latter method is more economical because the computation time varies linearly with the number of species.

17. Key Words (Suggested by Author(s))	18. Distribution Statement
Numerical method Reactive species Hypersonic flow	Unclassified - Unlimited Subject Category 02

19. Security Classif. (of this report)	20. Security Classif. (of this page)	21. No. of Pages	22. Price*
Unclassified	Unclassified	14	

*For sale by the National Technical Information Service, Springfield, Virginia 22161